Functional and physical interactions of components of the yeast mitochondrial inner-membrane import machinery (MIM)

Blom, J.; Dekker, P.J.T.; Meijer, M.

DOI
10.1111/j.1432-1033.1995.tb20813.x

Publication date
1995

Published in
European Journal of Biochemistry

Eur. J. Biochem. 232, 309–314 (1995)

Functional and physical interactions of components of the yeast mitochondrial inner-membrane import machinery (MIM)

Jolanda BLOM, Peter J. T. DEKKER and Michiel MEIJER

Section for Molecular Biology, Department of Molecular Cell Biology, BioCentrum Amsterdam, The Netherlands

(Received 4 May 1995) – EJB 95 0709/6

The essential mitochondrial inner-membrane protein, Mim44, is involved in the translocation of preproteins across the mitochondrial inner membrane. Two other putative components of this protein-translocation system are the integral inner-membrane proteins, Mim23 and Mim17. Here, we present genetic evidence for functional co-operation of all three proteins. Furthermore, we show that Mim23 and Mim17 are associated in a protein complex that also contains two proteins of 55 kDa and 20 kDa. We speculate that this subcomplex forms the proteinaceous import channel of the inner-membrane which transiently interacts with a less abundant peripheral complex of Mim44 and mitochondrial heat-shock protein Hsp70.

Keywords: mitochondrial inner membrane; protein import.

The majority of mitochondrial proteins are nuclear encoded and synthesized as preproteins on cytosolic ribosomes. The preproteins are imported into the mitochondrial matrix by independent proteinaceous translocation machineries in the mitochondrial outer and inner membranes. At least six proteins are members of the protein-translocation apparatus in the mitochondrial outer membrane in *Neurospora crassa* [1–6] and *Saccharomyces cerevisiae* [7–11].

Recent genetic and biochemical studies have identified three mitochondrial inner-membrane proteins, Mim44/Isp45 [12–14], Mim23/Mas6p [15, 16] and Mim17/Sms1p [17–19] as putative components of the inner-membrane protein-import system. Their involvement in preprotein import was indicated by crosslinking to a precursor protein spanning both mitochondrial membranes [13, 18, 20, 21] and by accumulation of unprocessed precursor proteins after depletion of any of the three proteins *in vivo* [12, 16, 19]. The role of the peripheral inner-membrane protein, Mim44, in translocation of preproteins is further indicated by (a) its preferential interaction with preproteins with a complete presequence [20], (b) inhibition of protein import into mitoplasts by Mim44 antiserum [13], and (c) biochemical and genetic evidence for an interaction with mitochondrial matrix heat-shock protein Hsp70 (mt-Hsp70), which has an established function in driving protein translocation [22–26]. Mim44 physically interacts with 10–20% mt-Hsp70, and this reversible association is controlled by ATP and preproteins.

Mim17 and Mim23 are both integral inner-membrane proteins and have significant sequence similarity in a region that contains putative membrane-spanning segments [15]. Current biochemical data support a similar membrane topology [15–17] and genetic data suggest a functional interaction between the two proteins [19]. It has been suggested that Mim17 and Mim23 might be integral components of the preprotein conducting channel of the inner-membrane [27], but no physical interaction has been shown so far.

Here, we present genetic evidence for a functional interaction of the preprotein-binding factor Mim44 with both Mim17 and Mim23. Furthermore, we show that Mim17 and Mim23 functionally and physically interact in a complex of proteins which also contains two proteins of 55 kDa and 20 kDa. We postulate that the mitochondrial inner-membrane import machinery may consist of two subcomplexes; a channel-forming core complex consisting of at least Mim17, Mim23, a 55-kDa protein and a 20-kDa protein, and a preprotein-binding complex formed by Mim44 and mt-Hsp70.

EXPERIMENTAL PROCEDURES

Strains and genetic procedures. *S. cerevisiae* strains used in this study are listed in Table 1. The *mim* mutants used in this study were derived from previously described import mutants [12, 15]. MB3-75 (*mim44-5*), MB3-33 (*mim17-1*), MB3-56 (*mim17-2*), MB3-81 (*mim17-3*), MB3-45 (*mim23-1*) and MB3-46 (*mim23-2*) were crossed with MB1; diploids were sporulated and his^-, trp^-, lys^-, leu^-, ura^- *mim* mutant spores were selected. Marker genes were integrated in the upstream non-coding regions of all *mim* alleles by transformation with DNA fragments containing one of the marker genes; MB75-9 and MB75-20 harbour the *LYS2* gene at the *Sna*BI site at position −556 relative to the start codon of the *mim44-5* allele. MB33-14, MB56-19 and MB81-20, contain the *TRP1* gene at the *Nsi*I site, 341-bp upstream of the start codon of the *mim17-1*, *mim17-2* and *mim17-3* alleles, respectively, and in MB45-1 and MB46-4 the *LEU2* gene at position −361 (*Spl*I site) relative to the start codon of the *mim23-1* and *mim23-2* alleles, respectively. Correct integration of all marker genes was verified by Southern-blot analysis. Yeast crosses, tetrad dissections and other genetic manipulations were performed by standard methods [28].

Mutant phenotypes were tested after transformation with the SOD-URA test plasmid encoding a chimeric protein with the mitochondrial-targeting sequence of superoxide dismutase and the *URA3* gene product [12]. The fusion protein is efficiently

Correspondence to M. Meijer, Section for Molecular Biology, Department of Molecular Cell Biology, BioCentrum Amsterdam, Kruislaan 318, 1098 SM Amsterdam, The Netherlands

Fax: +31 20 6685086.

Abbreviations. Mim, mitochondrial inner-membrane import machinery; mt-Hsp70, mitochondrial heat-shock protein Hsp70.

Table 1. *S. cerevisiae* strains used in this study.

Strain	Genotype	Source
MB1	*MATa his3 leu2 lys2-801 trp1-289 ura3-52*	[12]
MB3	*MATα ade2-101 his3-Δ200 leu2-Δ1 lys2-801 ura3::LYS2*	[12]
MB3-33	*MATα ade2-101 his3-Δ200 leu2-Δ1 lys2-801 ura3::LYS2 mim17-1*	[15]
MB3-56	*MATα ade2-101 his3-Δ200 leu2-Δ1 lys2-801 ura3::LYS2 mim17-2*	[15]
MB3-81	*MATα ade2-101 his3-Δ200 leu2-Δ1 lys2-801 ura3::LYS2 mim17-3*	[15]
MB3-45	*MATα ade2-101 his3-Δ200 leu2-Δ1 lys2-801 ura3::LYS2 mim23-1*	[15]
MB3-46	*MATα ade2-101 his3-Δ200 leu2-Δ1 lys2-801 ura3::LYS2 mim23-2*	[15]
MB3-75	*MATα ade2-101 his3-Δ200 leu2-Δ1 lys2-801 ura3::LYS2 MIM44-5*	[15]
MB33-14	*MATa ade2-101 his3 leu2 lys2-801 trp1-289 ura3-52 mim17-1(TRP1)*	this study
MB56-19	*MATa ade2-101 his3 leu2 lys2-801 trp1-289 ura3-52 mim17-2(TRP1)*	this study
MB81-21	*MATa ade2-101 his3 leu2 lys2-801 trp1-289 ura3-52 mim17-3(TRP1)*	this study
MB45-1	*MATα ade2-101 his3 leu2 lys2-801 trp1-289 ura3-52 mim23-1(LEU2)*	this study
MB46-4	*MATα ade2-101 his3 leu2 lys2-801 trp1-289 ura3-52 mim23-2(LEU2)*	this study
MB75-9	*MATa his3 leu2 lys2-801 trp1-289 ura3-52 mim44-5(LYS2)*	this study
MB75-20	*MATα his3 leu2 lys2-801 trp1-289 ura3-52 mim44-5(LYS2)*	this study
MB16	*ade2-101 his3 leu2 lys2-801 trp1-289 ura3-52 mim17::Lys2 + YCplac111::MIM17-c-myc (LEU2)*	[17]

imported into mitochondria, and wild-type cells with a nuclear ura3 mutation and harbouring the test plasmid are still unable to grow in the absence of exogenously added uracil. Since, in *mim* mutants, mitochondrial import of the SOD-URA fusion protein is at least partially blocked, the fusion protein will restore cytosolic pyrimidine synthesis and thus allows cells to grow in uracil-free medium.

Cloning procedures. Recombinant DNA methods were performed according to standard procedures [29]. YCplac33::-*MIM44* contains a 2.7-kb *Hin*dIII fragment harbouring the *MIM44* gene [12]. YCplac33::*MIM23* contains an 1818-bp *Sph*I fragment harbouring the *MIM23* gene [15]. YCplac33::*MIM17* contains a 1158-bp *Eco*RI–*Bam*HI fragment harbouring the *MIM17* gene derived from YCplac111::*MIM17*(*Bst*EII/*Hin*cII), which contains a 1137-bp *Bst*EII–*Hin*cII fragment containing *MIM17* [17]. To generate YCplac111::*MIM17*(*TRP1*), an 828-bp *Eco*RI–*Stu*I *TRP1* fragment from YRP7 [30] was blunted and inserted into the blunted *Nsi*I site in YCplac111::*MIM17*(*Xba*I/*Sal*I; Maarse et al., 1994), 341 bp upstream of the coding sequence of *MIM17* [17]. A 1699-bp *Bam*HI–*Bst*EII fragment of YCplac111::*MIM17*(*TRP1*), containing the *TRP1* gene flanked by 5′-noncoding sequences of *MIM17*, was used for transformation of the *mim17* mutants. *Mim44* mutants were transformed with a DNA fragment containing the *LYS2* gene flanked by 5′-noncoding sequences of *MIM44*, which was isolated by liberating a 5784-bp *Hin*dIII–*Eco*RI fragment from pUC18::*MIM44* (*LYS2*). To generate pUC18::*MIM44*(*LYS2*), an 898-bp *Hin*dIII–*Spe*I *MIM44* fragment from YEplac181::*MIM44*, which contains a 2.7-kb *Hin*dIII fragment carrying *MIM44* [12], was inserted into the *Hin*dIII–*Xba*I cloning sites of pUC18 [31], followed by insertion of a 4875-bp blunted *Hin*dIII *LYS2* fragment from pDP6 [32] into the *Sna*BI site of *MIM44*, 556 bp upstream of the start codon of *MIM44* [12]. A 2478-bp *Hpa*I–*Sma*I fragment from pUC18::*MIM23*(*LEU2*) was isolated to transform the *mim23* mutants with the *LEU2* gene flanked by 5′-noncoding sequences of *MIM23*. pUC18::*MIM23*(*LEU2*) was constructed by cloning a 911-bp *Pst*I fragment of YEplac181::*MIM23* (containing a 1.6-kb *Sph*I fragment harbouring the *MIM23* gene [15]) into the *Pst*I site of pUC18 and subsequent insertion of a 1974-bp *Hpa*I–*Sal*I blunted *LEU2* fragment from construct 6 [33] into the blunted *Spl*I site of *MIM23*, 361-bp upstream of the start codon of *MIM23* [15].

^{35}S labelling of mitochondria. ^{35}S labelling of yeast cells was according to the procedure of Kolodziej and Young [34]. A culture of yeast strain MB16 [17] in synthetic lactate medium was diluted 50 times in low-sulphate medium (LSM [35]), containing 0.02 mM $(NH_4)_2SO_4$, required amino acids and 2% lactate as carbon source, and shaken at 28 °C to an A_{600} of about 1. Cells were harvested (about 200 mg wet mass), washed once in sterile water, then vigorously shaken for 5 min at room temperature in the presence of 5 mCi [^{35}S]sulphate (Amersham) in a volume of 100 µl. The cell suspension was diluted with 5 ml LSM and shaken for 30 min at 28 °C. After the addition of 25 ml LSM containing 0.02 mM $(NH_4)_2SO_4$, the culture was shaken for another 3–4 h until the uptake of [^{35}S]sulphate by the cells was approximately 50–80%. Cells were harvested and washed once with ice-cold breaking buffer (0.6 M sorbitol, 20 mM Tris/Cl, pH 7.4, 0.5 mM EDTA, 1 mM phenylmethylsulfonyl fluoride). Submitochondrial particles (mitochondrial membranes) were isolated by lysis of the yeast cells with glass beads in breaking buffer and differential centrifugation, as described [36]. The specific activity of the final membrane preparation was approximately 0.2 Ci/g protein.

Immune precipitations. ^{35}S-labelled mitochondrial particles (0.01 mCi/sample) were suspended in 0.1 ml ice-cold lysis buffer [0.1% Triton X-100 (BDH) or 1% digitonin (Kodak), 20 mM Tris/Cl, pH 7.4, 0.1 mM EDTA, 50 mM NaCl, 10% glycerol, 1 mM phenylmethylsulfonyl fluoride]. After centrifugation at 30000 *g* for 15 min, the supernatants were added to antibodies bound to protein-A–Sepharose (Pharmacia), diluted to 0.4 ml with lysis buffer, and gently shaken at 8 °C for 1 h. Subsequently, the Sepharose beads were harvested and washed three times with 1 ml lysis buffer. The co-precipitating proteins were analyzed by SDS/PAGE, Western blotting and autoradiography. For a second immune precipitation under denaturing conditions, the immune complexes were dissociated in 0.02 ml 2% SDS for 2 min at 90 °C, dwith a 25-fold excess of 1% Triton X-100, 20 mM Tris/Cl, pH 7.4, 5 mM EDTA, 150 mM NaCl and subjected to immune precipitation as described above. The presence of Mim17 in the Mim complex was established by solubilization of 1 mg MB16 mitochondria in 1 ml lysis buffer, immune precipitation with anti-Mim23 or pre-immune serum, and decoration of Western blots with monoclonal anti-(c-myc) (Cambridge Research Biochemicals). Mim17–c-myc was visualized with horseradish peroxidase coupled to goat-anti-mouse IgG (BioRad).

Steady-state expression analysis of Mim44, Mim23 and Mim17. MB3 was transformed with the plasmids YCplac111::-*MIM44*-c-myc [12], YCplac111::*MIM23*-c-myc [24] or YC-

plac111::*MIM17*-c-myc[17], that express a human c-myc epitope at the carboxy terminus of each protein. Transformants were grown in synthetic lactate medium until A_{600} was 5. Total protein lysates were prepared by shaking with glass beads in the presence of 5% trichloroacetic acid and precipitated proteins were pelleted and dissolved in SDS-containing sample buffer, subjected to SDS/PAGE and Western blotting. Expression of the plasmid-borne genes was compared with expression of the nuclear-encoded genes by immune decoration of blots with anti-Mim44 or anti-Mim23. Expression of the c-myc-tagged Mim proteins was monitored by immune decoration with anti-(c-myc).

RESULTS

Functional interaction between Mim44, Mim23 and Mim17. Mim44, Mim17 and Mim23 can each be crosslinked to a preprotein in transit across the mitochondrial membranes [18], suggesting that they are involved in preprotein import and might function at the same import site of a translocating preprotein. However, no simultaneous crosslinking of the three proteins to one type of translocation intermediate has been observed. To obtain independent evidence for a functional connection between Mim44, Mim23 and Mim17, we therefore tested whether or not strains with double *mim* mutations are inviable. Combinations of mild mutations in two different but functionally related genes can cause such a synthetic lethal phenotype. Synthetic lethality is regarded as valid genetic evidence for a functional interaction between gene products [37–44].

The *mim44* mutant MB3-75, the *mim23* mutants MB3-45 and MB3-46, and the *mim17* mutants MB3-33, MB3-56 and MB3-81 [12, 15] were crossed with the wild-type strain MB1, diploids were sporulated and haploids containing a *mim* allele and a set of auxotrophic markers were selected. To facilitate segregation analysis of mutant alleles in the test for synthetic lethality, the *mim* alleles of these haploid strains were marked by integration of either the *LYS2* gene, the *TRP1* gene or the *LEU2* gene in the upstream non-coding region. All haploids with marked *mim* alleles exhibited the same phenotype as the ancestral mutants with a partial import defect. Due to the leakiness of the single *mim* mutations, the mutant strains grow well at 23°C on both fermentable and non-fermentable carbon sources.

Crosses were performed between the marked *mim* mutant haploids. Heterozygous diploids containing pairwise combinations of the three marked *mim* alleles were sporulated, tetrads dissected and spores grown for 5–6 days on glucose-containing medium at 23°C. Colonies were then replica plated to determine the segregation pattern of the marked mutant alleles in viable spores of each tetrad. Spores derived from the heterozygous *mim17-mim23* diploids were tested for the presence of the *TRP1* and/or the *LEU2* markers (Table 2). Viable spores containing both marker genes were virtually absent, indicating that combinations of the *mim17* and *mim23* mutations caused inviability. A similar result was found for spores derived from the heterozygous *mim44-mim17* diploid (Table 3) and the heterozygous *mim44-mim23* diploid (Table 4); in all cases, hardly any spores containing two marker genes were present. Therefore, the segregation analysis of the different marked mutant *mim* alleles indicate a synthetic lethal effect of all pairwise combinations of mutant alleles of *MIM44*, *MIM23* and *MIM17*.

A few tetrads of different crosses yielded spores with markers of both *mim* alleles. However, these tetrads also yielded spores lacking both marker genes but harbouring at least one *mim* mutant allele. We presume that, in these rare cases, a meiotic recombination event has occurred which caused unlinking of a particular marker gene and the *mim* allele. The few viable spores with double marker genes were therefore disregarded.

When heterozygous diploids were first transformed with the centromeric plasmid YCplac33 containing a wild-type copy of one of both *mim* alleles, then sporulated, about 25% of plasmid-containing spores harboured both marked mutant alleles (Tables 2–4). This shows that the synergistic lethal effect can be abolished by introduction of a wild-type *MIM* gene, meaning that it is a direct consequence of the presence of two *mim* mutations. Since all pairwise combinations of mutations in the three different *MIM* genes caused synthetic lethality, we conclude that Mim44, Mim23 and Mim17 functionally interact.

Physical interactions within the inner-membrane import system. To investigate physical interactions of the previously identified Mim proteins and to identify additional components of the putative Mim complex, we performed immune precipitations with antibodies raised against Mim23 [18]. A yeast strain with a deletion of the chromosomal *MIM17* gene and harbouring a centromeric plasmid expressing Mim17 furnished with a carboxy-terminal c-myc epitope was used for this analysis [17]. Mim17–c-myc fully complements the deletion of the endogenous *MIM17* gene, indicating its correct assembly in the mitochondrial inner membrane. Mitochondrial particles were isolated from this strain after growth in [^{35}S]sulphate-containing medium. Mitochondrial membranes were solubilized with 0.1% Triton X-100 or 1% digitonin and immune precipitations were performed with antibodies raised against Mim23, Mim44 or the

Table 2. Genetic interaction between MIM23 and MIM17. Heterozygous double *mim23/mim17* mutant diploids were sporulated, tetrads dissected and spores grown for 5–6 days at 23°C. Colonies were then replica plated to determine the segregation of the *LEU2* and *TRP1* marked mutant alleles. One diploid was transformed with the centromeric plasmid YCplac33 containing a wild-type copy of either *MIM17* or *MIM23* before sporulation. In these cases, only plasmid-containing spores were analysed.

Cross	Plasmid	Number of viable spores with *LEU2/TRP1* marked mutant alleles			
		total	0 markers	one marker	two markers
mim23-1(LEU2) × *mim17-3(TRP1)*	–	49	19	29	1
× *mim17-2(TRP1)*	–	57	17	40	0
× *mim17-1(TRP1)*	–	34	8	25	1
mim23-2(LEU2) × *mim17-3(TRP1)*	–	59	21	38	0
× *mim17-2(TRP1)*	–	46	14	32	0
× *mim17-1(TRP1)*	–	40	9	31	0
× *mim17-1(TRP1)*	YCplac33::*MIM17*	30	4	16	10
× *mim17-1(TRP1)*	YCplac33::*MIM23*	25	7	14	4

Table 3. Genetic interaction between MIM44 and MIM17. Heterozygous double *mim44/mim17* mutant diploids were sporulated, tetrads dissected and spores grown for 5–6 days at 23°C. Colonies were then replica plated to determine the segregation of the *LYS2* and *TRP1* marked mutant alleles. One diploid was transformed with the centromeric plasmid YCplac33 containing a wild-type copy of either *MIM44* or *MIM17* before sporulation. In these cases, only plasmid-containing spores were analysed.

Cross	Plasmid	Number of viable spores with *LYS2/TRP1* marked mutant alleles			
		total	0 markers	one marker	two markers
mim44-5(LYS2) × *mim17-3(TRP1)*	–	44	16	27	1
× *mim17-2(TRP1)*	–	51	12	38	1
× *mim17-1(TRP1)*	–	79	21	58	0
× *mim17-1(TRP1)*	YCplac33::*MIM17*	31	6	17	8
× *mim17-1(TRP1)*	YCplac33::*MIM44*	30	8	15	7

Table 4. Genetic interaction between MIM44 and MIM23. Heterozygous double *mim44/mim23* mutant diploids were sporulated, tetrads dissected and spores grown for 5–6 days at 23°C. Colonies were then replica plated to determine the segregation of the *LYS2* and *LEU2* marked mutant alleles. One diploid was transformed with the centromeric plasmid YCplac33 containing a wild-type copy of either *MIM44* or *MIM23* before sporulation. In these cases only plasmid-containing spores were analysed.

Cross	Plasmid	Number of viable spores with *LYS2/LEU2* marked mutant alleles			
		total	0 markers	one marker	two markers
mim44-5(LYS2) × *mim23-1(LEU2)*	–	59	23	35	1
× *mim23-2(LEU2)*	–	51	22	27	2
× *mim23-2(LEU2)*	YCplac33::*MIM23*	22	7	9	6
× *mim23-2(LEU2)*	YCplac33::*MIM44*	38	12	13	13

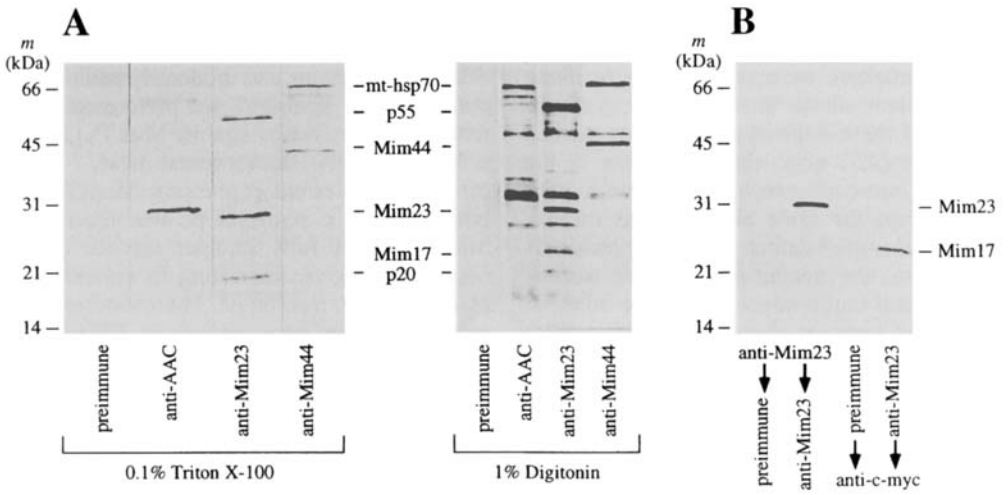

Fig. 1. Immune precipitation of the Mim complex. (A) ^{35}S-labelled yeast mitochondria isolated from strain MB16 were lysed in Triton X-100-containing (left panel) or digitonin-containing (right panel) buffer and proteins were precipitated with antibodies coupled to protein-A–Sepharose. Precipitated material was analyzed by SDS/PAGE, blotted, and proteins visualized by autoradiography. (B) Left two lanes, material precipitated with anti-Mim23 was re-solubilized in 2% SDS and re-precipitated with pre-immune serum or anti-Mim23 and further analysed as described above; right two lanes, lysed mitochondria (about 1 mg protein) were precipitated with pre-immune serum or anti-Mim23. Precipitated proteins were subjected to SDS/PAGE, blotted onto nitrocellulose and the presence of Mim17–c-myc was established by immmune decoration with antibodies against a human c-myc epitope.

abundant mitochondrial inner-membrane protein ADP/ATP carrier. Three proteins with apparent molecular masses of 55, 29 and 20 kDa, were specifically precipitated with Mim23 antiserum, both after solubilizing the membranes with digitonin or with Triton X-100 (Fig. 1A). The precipitated complex from digitonin-solubilized mitochondria contains, in addition, a protein with apparent molecular mass of 22 kDa (Fig. 1A). Other co-precipitating bands are regarded as non-specific, since they are also precipitated by pre-immune serum or antiserum against the ADP/ATP carrier. The antiserum against the highly abundant inner-membrane ADP/ATP carrier did not precipitate the 55-, 29-, 20- and 22-kDa proteins, indicating that their co-precipitation with Mim23 represents a specific association and is not due to incomplete solubilization of large and non-specific membrane complexes. When the precipitated complex was solubilized in an SDS-containing buffer and re-precipitated with anti-Mim23,

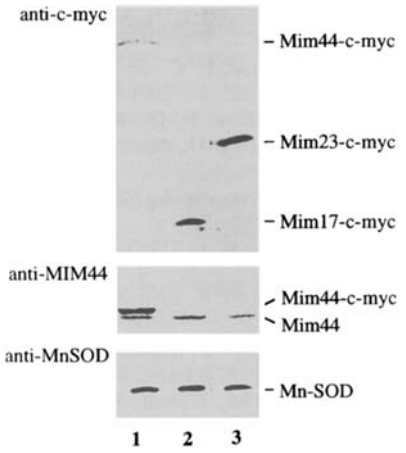

Fig. 2. Stoichiometry of the different Mim proteins. Mim44, Mim17 and Mim23, harbouring a carboxy-terminal c-myc epitope, were expressed from a centromeric plasmid in the wild-type yeast strain MB3. Total protein extracts (0.2 mg/lane) were subjected to SDS/PAGE and Western blotting. Lane 1, MB3 expressing Mim17−c-myc; lane 2, MB3 expressing Mim23−c-myc;. lane 3, MB3 expressing Mim44−c-myc. C-myc-tagged proteins were visualized by immmune decoration with anti-(c-myc). To compare the steady-state level of endogenous Mim44 with plasmid-encoded Mim44−c-myc, the same blot was incubated with anti-Mim44. As a control for the amount of layered material, the same blot was decorated with antibodies raised against yeast mitochondrial manganese superoxide dismutase (anti-MnSOD).

only the 29-kDa band was precipitated, identifying this band as Mim23 (Fig. 1B). Furthermore, SDS/polyacrylamide gel electrophoresis of the precipitated complex, subsequent Western blotting and immune decoration with monoclonal antibodies against the c-myc epitope, identified unequivocally the 22-kDa band as Mim17−c-myc (Fig. 1B). The estimated molecular masses of Mim23 and Mim17 on SDS/PAGE deviate considerably from the calculated molecular masses of these proteins, a phenomenon frequently observed for hydrophobic membrane proteins.

The Mim complex is highly labile, even after solubilization of membranes with low concentrations of the mild detergents. Mim17 only remains associated with the complex when membranes are solubilized with digitonin. Mim44 and associated mt-Hsp70 were not present in the complex, irrespective of whether digitonin or Triton X-100 was used, and none of the proteins of the complex could be precipitated with the Mim44 antiserum (Fig. 1A). We conclude that a possible physical interaction with the peripheral Mim44/mt-Hsp70 subcomplex must be highly labile or exists only transiently. The results indicate that the integral inner-membrane proteins Mim23 and Mim17 are associated in one complex in the mitochondrial inner-membrane and that this subcomplex contains two additional proteins of 55 kDa and 20 kDa (p55 and p20, respectively).

Stoichiometry of Mim44, Mim23 and Mim17. Above, we have shown a functional interaction between Mim17, Mim23 and Mim44. A physical association of these proteins was, however, only observed for Mim17 and Mim23, suggesting that the inner-membrane protein-translocation system may consist of several subcomplexes. We, therefore, studied whether steady-state expression levels of the Mim proteins could give an indication of the relative abundance of the putative Mim44/mt-Hsp70 subcomplex and the putative subcomplex containing Mim23 and Mim17.

The wild-type yeast strain MB3 was transformed with a centromeric plasmid expressing Mim44, Mim23 or Mim17 from their own promoters and all with a c-myc epitope at their carboxy termini. The three proteins could, therefore, be detected with the same anti-(c-myc), allowing direct comparison of their expression levels. Each c-myc-tagged protein complements the corresponding deletion mutant, indicating that all three fusion proteins are functional and are assembled correctly in the inner membrane. After growth of the transformed MB3 cells on synthetic-lactate containing medium to a similar cell density, total cell lysates were analysed by SDS/PAGE and Western blotting. Immune decoration with anti-Mim44 (Fig. 2) or anti-Mim23 (not shown) indicated approximately equal expression levels of a tagged Mim protein and its nuclear-encoded counterpart. When the blot was decorated with anti-(c-myc), the steady-state level of Mim44 was approximately 5−10-times lower than that of either Mim23 or Mim17 (Fig. 2). The comparable expression levels of Mim23 and Mim17 suggest that Mim17 and Mim23 have a 1:1 stoichiometry in the Mim complex, while the putative subcomplex of Mim44/mt-Hsp70 is 5−10-times less abundant.

DISCUSSION

In this report, we present evidence for physical and functional interactions between the previously identified Mim components of the putative preprotein-translocation system in the yeast mitochondrial inner membrane. The data suggest that this system may consist of two subcomplexes; one integrally embedded in the inner-membrane and composed of at least four subunits (Mim17, Mim23, p20 and p55), and one peripherally associated with the inner-membrane and consisting of Mim44 and mt-Hsp70 [24−26]. We propose that the Mim17/Mim23/p20/p55 subcomplex forms the protein-conducting channel in the mitochondrial inner membrane. The identity and topology of the new putative members of this channel (p55 and p20) are at present unknown, but p55 might be identical to the 60-kDa protein that co-precipitated with Mas6p/Mim23 when mitochondrial membranes were solubilized with 1% Triton X-100 after crosslinking to a Su9-dihydrofolate-reductase translocation intermediate [21]. Correspondingly, we found that p55 remains associated with Mim23 under these solubilization conditions (Dekker, P. J. T., unpublished results). The immune precipitation experiments further showed that the integrally embedded Mim complex did not stably associate with Mim44 in the presence of any of the detergents tested. However, crosslinking of Mim44, Mim23 and Mim17 to the same type of translocation intermediate of Su9-dihydrofolate-reductase suggests that these proteins might function at the same import site [24]. Here, we provide independent evidence for a functional interaction between Mim44, Mim23 and Mim17 by showing synthetic lethality between different mutant alleles of all three *MIM* genes.

One explanation for the synergism between mutations in the two genes could be that the inviability of the double mutants is due to the cumulated defects caused by mutations in unrelated genes. This explanation is very unlikely in the case of double *mim* mutants since single *mim* mutants are very leaky and their growth is indistinguishable from that of wild-type cells. Moreover, in several cases, synthetic lethal phenotypes are caused by two mutant gene products which interact in the same pathway. Examples are combinations of *sec* mutations blocking secretory-protein transport from the endoplasmic reticulum to the Golgi apparatus [38, 40] and mutations affecting protein delivery to the cell surface [41]. In these cases, synthetic lethal phenotypes are exclusively found in combinations of mutant gene products acting at the same stage of the secretory pathway. The synthetic growth defect of strains mutated in both *MIM44* and *SSC1*, the

gene encoding mt-Hsp70, repesents another example [24]. In other cases of synergism between mutations, the gene products appeared to function not in the same pathway but in parallel routes [45]. The existence of by-pass routes is unlikely in our case, since a null mutation in any of the genes is lethal and the different Mim proteins cannot substitute each other. We, therefore, favour the interpretation that Mim44, Mim23 and Mim17 functionally interact in the same translocation apparatus of the inner membrane.

The difference in abundance of Mim44 and Mim23/Mim17 may be explained in two different ways. First, each inner-membrane translocation channel may contain multiple copies of Mim23 and Mim17. This could mean that mitochondria have sufficient Mim44 to occupy all translocation pores, and that both subcomplexes are present in equimolar amounts. Since Mim44 does not form a detectable stable interaction with the Mim23/Mim17 subcomplex, we prefer another possibility. In this case, each protein-conducting channel contains only one subunit of Mim17 and Mim23 and the number of channels exceeds the number of Mim44/mt-Hsp70 subcomplexes. This could imply that Mim44 cycles between different Mim17/Mim23-containing translocation channels. Since Mim44 is involved in an early step in the translocation process and interacts predominantly with preproteins carrying a complete presequence [20], Mim44 might only be required for translocation of the presequence across the inner membrane. After initial binding to Mim44, the translocating preprotein is transferred to mt-Hsp70, which may trap the presequence of the preprotein in the matrix and initiates the $\Delta\psi$-independent translocation of the mature part of the protein. Mt-Hsp70 drives further translocation of the protein through the import channel, even after dissociation from Mim44. Mim44 is therefore no longer required and can be laterally moved to another import channel to initiate translocation of another preprotein, thereby recruiting new mt-Hsp70 from the matrix space. While cycling of mt-Hsp70 between a soluble and Mim44-bound state is regulated by ATP hydrolysis [24–26], we can only speculate about the cycling mechanism of the permanently membrane-associated Mim44 between different translocation channels and the possible involvement of Mim proteins or yet unidentified inner-membrane proteins in this dynamic process.

We are grateful to A. C. Maarse, N. Pfanner and L. A. Grivell for helpful discussions and comments on the manuscripts. We thank M. de Jong for expert technical assistance.

REFERENCES

1. Söllner, T., Griffiths, G., Pfaller, R., Pfanner, N. & Neupert, W. (1989) *Cell 59*, 1061–1070.
2. Söllner, T., Pfaller, R., Griffiths, G., Pfanner, N. & Neupert, W. (1990) *Cell 62*, 107–115.
3. Söllner, T., Rassow, J., Wiedmann, M., Schlossmann, J., Keil, P., Neupert, W. & Pfanner, N. (1992) *Nature 355*, 84–87.
4. Kiebler, M., Pfaller, R., Söllner, T., Griffiths, G., Horstmann, H., Pfanner, N. & Neupert, W. (1990) *Nature 348*, 610–616.
5. Kiebler, M., Keil, P., Schneider, H., Van der Klei, I. J., Pfanner, N. & Neupert, W. (1993) *Cell 74*, 483–492.
6. Keil, P. & Pfanner, N. (1993) *FEBS Lett. 321*, 197–200.
7. Hase, T., Riezman, H., Suda, K. & Schatz, G. (1983) *EMBO J. 2*, 2169–2172.
8. Baker, K. P., Schaniel, A., Vestweber, D. & Schatz, G. (1990) *Nature 348*, 605–609.
9. Hines, V., Brandt, A., Griffiths, G, Horstmann, H., Brutsch, H. & Schatz, G. (1990) *EMBO J. 9*, 3191–3200.
10. Moczko, M., Dietmeier, K., Söllner, T., Segui, B., Steger, H. F., Neupert, W. & Pfanner, N. (1992) *FEBS Lett. 310*, 265–268.
11. Ramage, L., Junne, T., Hahne, K., Lithgow, T. & Schatz, G. (1993) *EMBO J. 12*, 4115–4123.
12. Maarse, A. C., Blom, J., Grivell, L. A. & Meijer, M. (1992) *EMBO J. 11*, 3619–3628.
13. Scherer, P. E., Manningkrieg, U. C., Jeno, P., Schatz, G. & Horst, M. (1992) *Proc. Natl Acad. Sci. USA 89*, 11930–11934.
14. Horst, M., Jeno, P., Kronidou, N. G., Bolliger, L., Oppliger, W., Scherer, P., Manning-Krieg, U., Jascur, T. & Schatz, G. (1993) *EMBO J. 12*, 3035–3041.
15. Dekker, P. J. T., Keil, P., Rassow, J., Maarse, A. C. & Meijer, M. (1993) *FEBS Lett. 330*, 66–70.
16. Emtage, J. L. T. & Jensen, R. E. (1993) *J. Cell Biol. 122*, 1003–1012.
17. Maarse, A. C., Blom, J., Keil, P., Pfanner, N. & Meijer, M. (1994) *FEBS Lett. 349*, 215–221.
18. Kübrich, M., Keil, P., Rassow, J., Dekker, P. J. T., Blom, J., Meijer, M. & Pfanner, N. (1994) *FEBS Lett. 349*, 222–228.
19. Ryan, K. R., Menold, M. M., Garrett, S. & Jensen, R. E. (1994) *Mol. Biol. Cell 5*, 529–538.
20. Blom, J., Kübrich, M., Rassow, J., Voos, W., Dekker, P. T. J., Maarse, A. C., Meijer, M. & Pfanner, N. (1993) *Mol. Cell. Biol. 13*, 7364–7371.
21. Ryan, K. R. & Jensen, R. E. (1993) *J. Biol. Chem. 268*, 23743–23746.
22. Kang, P. J., Ostermann, J., Shilling, J., Neupert, W., Craig, E. A. & Pfanner, N. (1990) *Nature 348*, 137–143.
23. Gambill, B. D., Voos, W., Kang, P. J., Miao, B. J., Langer, T., Craig, E. A. & Pfanner, N. (1993) *J. Cell Biol. 123*, 109–117.
24. Rassow, J., Maarse, A. C., Krainer, E., Kübrich, M., Müller, H., Meijer, M., Craig, E. A. & Pfanner, N. (1994) *J. Cell Biol. 127*, 1547–1556.
25. Schneider, H. C., Berthold, J., Bauer, M. F., Dietmeier, K., Guiard, B., Brunner, M. & Neupert, W. (1994) *Nature 371*, 768–774.
26. Kronidou, N. G., Oppliger, W., Bolliger, L., Hannavy, K., Glick, B. S., Schatz, G. & Horst, M. (1994) *Proc. Natl Acad. Sci. USA 91*, 12818–12822.
27. Pfanner, N., Craig, E. A. & Meijer, M. (1994) *Trends Biochem. Sci. 19*, 368–372.
28. Sherman, F., Fink, G. R. & Hicks, J. B. (1986) *Methods in yeast genetics*, Cold Spring Harbor Laboratory, Cold Spring Harbor, NY.
29. Sambrook, J., Fritsch, E. F. & Maniatis, T. (1989) *Molecular cloning, a laboratory manual*, 2nd edn, Cold Spring Harbor Laboratory, Cold Spring Harbor, NY.
30. Struhl, K., Stinchcomb, D. T., Scherer, S. & Davis, R. W. (1979) *Proc. Natl Acad. Sci. USA 76*, 1035–1039.
31. Yanish-Perron, C., Vieira, J. & Messing, J. (1985) *Gene (Amst.) 33*, 103–119.
32. Fleig, U. N., Pridmore, R. D. & Philippsen, P. (1986) *Gene (Amst.) 46*, 237–245.
33. Maarse, A. C., de Haan, M., Schoppink, P. J., Berden, J. A. & Grivell, L. A. (1988) *Eur. J. Biochem. 172*, 179–184.
34. Kolodziej, P. A. &. Young, R. A. (1991) *Methods Enzymol. 194*, 508–519.
35. Fox, T. D., Folley, L. S., Mulero, J. J., McMullin, T. W., Thorsness, P. E., Hedin, L. O. & Constanzo, M. C. (1991) *Methods Enzymol. 194*, 149–165.
36. Douglas, M., Finkelstein, D. & Butow, R. A. (1979) *Methods Enzymol. 56*, 58–66.
37. Huffaker, T. C., Hoyt, M. A. & Botstein, D. (1987) *Annu. Rev. Genet. 21*, 259–284.
38. Rothblatt, J. A., Deshaies, R. J., Sanders, S. L., Daum, G. & Schekman, R. (1989) *J. Cell Biol. 109*, 2641–2652.
39. Bender, A. & Pringle, J. R. (1991) *Mol. Cell. Biol. 11*, 1295–1305.
40. Kaiser, C. A. & Schekman, R. (1990) *Cell 61*, 723–733.
41. Salminen, A. & Novick, P. J. (1987) *Cell 49*, 527–538.
42. Wimmer, C., Doye, V., Grandi, P., Nehrbass, U. & Hurt, E. C. (1992) *EMBO J. 11*, 5051–5061.
43. Holtzman, D. A., Yang, S. & Drubin, D. G. (1993) *J. Cell Biol. 122*, 635–644.
44. Berges, T., Petfalski, E., Tollervey, D. & Hurt, E. C. (1994) *EMBO J. 13*, 3136–3148.
45. Haynes, R. H. & Kunz, B. A. (1978) *DNA repair and mutagenesis in yeast*, Cold Spring Harbor Laboratory, Cold Spring Harbor, NY.